

Supplementary Information

Stability of oxylipins during plasma generation and long-term storage

Elisabeth Koch^{*,1}, Malwina Mainka^{*,1}, Céline Dalle², Annika I. Ostermann¹, Katharina M. Rund¹,
Laura Kutzner¹, Laura-Fabienne Froehlich¹, Justine Bertrand-Michel³, Cécile Gladine², Nils
Helge Schebb^{#,1}

¹Chair of Food Chemistry, Faculty of Mathematics and Natural Sciences, University of Wuppertal,
Wuppertal, Germany

²Université Clermont Auvergne, INRA, UNH, Unité de Nutrition Humaine, CRNH Auvergne, Clermont-
Ferrand, France

³MetaToul, Inserm/UPS UMR 1048 - I2MC, Institut des Maladies Métaboliques et Cardiovasculaires,
Toulouse, France

*Authors contributed equally.

#Contact information for corresponding author:

Nils Helge Schebb
Chair of Food Chemistry
Faculty of Mathematics and Natural Sciences
University of Wuppertal
Gaußstr. 20
42119 Wuppertal
nils@schebb-web.de
Tel: +49-202-439-3457

Table of Contents

Preparation of oxylipin standard series.....	2
Sample preparation	3
Table S1.....	4
Table S2.....	9
Table S3.....	10
Table S4.....	11
Table S5.....	12
Table S6.....	12
Table S7.....	12
Figure S1.....	13
Figure S2.....	14
Figure S3.....	15
Figure S4.....	16
Figure S5.....	17
Figure S6.....	18
Figure S7.....	19
Figure S8.....	22
Figure S9.....	23
Figure S10.....	24

Preparation of oxylipin standard series

Oxylipins were combined to master mixes according to their molecular weight and sufficient chromatographic separation (Table S1). Master mixes were prepared in a volumetric flask (5 mL) with a tentative concentration of 10 μ M based on the declaration of the manufacturer. Due to limited available standard material the regioisomers of EpODE and DiHODE, 9(10)-EpOME, 7(8)-EpDPE, 8,15-DiHETE, 5(S),6(S)-DiHETE, 8-HETE, 9-HETE and 11-HETE have been added at lower concentrations

The IS master was prepared in a volumetric flask (25 mL) with a tentative concentration of 5 μ M. The internal standards $^2\text{H}_5\text{-RvD1}$ and $^2\text{H}_4\text{-PGB}_2$ were added at lower concentration because of their contamination with unlabeled isotopologs. The IS master was diluted with MeOH to a 100 nM “*sample preparation IS*”-solution in a volumetric flask and aliquoted in amber vials until use.

The purity and the concentration of the analytes in the master mixes was checked before pipetting the standard series (Figure S1).

All oxylipin solutions were prepared avoiding direct light radiation, using only detergent free glassware (no plastic) and stored at -80°C.

Determination of standard purity and verification of concentration

All master mixes were analyzed by means of LC-MS/MS in multiple reaction monitoring (MRM) mode. All transitions of not included analytes were evaluated for contamination/interferences. For detected interferences the standard compound containing the interference was identified. The contamination was quantified by calculating an area ratio between the contamination (at 5 μ M) and the analyte standard at 5 μ M. If an area ratio was higher than 10%, the contaminated oxylipin was removed from the standard series.

The master mixes were analyzed by means of LC-MS in single ion monitoring (SIM) mode and by means of UV spectroscopy according to Hartung *et al.*, 2019 (Prostag Oth Lipid M 141, 22-24). The actual analyte concentration was adjusted by comparison with concentration-verified standard material.

Preparation of standard series

Calibrants with 16 concentrations levels were prepared by a sequential dilution with IS master (Table S2). The internal standards concentrations were 20 nM, except for $^2\text{H}_5$ -RvD1 and $^2\text{H}_4$ -PGB₂ (5 nM and 10 nM in calibrants, respectively).

For calibration the peak area ratio (analyte/IS) was linearly fitted against the analyte concentration using linear least square regression (weighting $1/x^2$) (SI Table S3). The concentration with a signal to noise ratio of ≥ 3 was determined as limit of detection (LOD). The lower limit of quantification (LLOQ) was set to the concentration yielding a signal to noise ratio of ≥ 5 and accuracy of $\pm 20\%$ within the calibration curve. The accuracy within the calibration curve was $\pm 15\%$ fulfilling the validation criteria of the European Medicines Agency (EMA) guideline for bioanalyses (Agency, E. M. In *EMA/CHMP/EWP/192217/2009 Rev. 1 Corr. 2*, 2011).

Sample preparation

To 100 μ L thawed plasma 10 μ L of IS solution (100 nM in MeOH) and 10 μ L of antioxidant mixture (0.2 mg/mL BHT, 100 μ M indomethacin, 100 μ M trans-4-(-4-(3-adamantan-1-yl-ureido)-cyclohexyloxy)-benzoic acid (*t*-AUCB) in MeOH) were added. For protein precipitation 400 μ L ice-cold *iso*-propanol was added and the samples were stored at -60°C for at least 30 min. Following centrifugation (4°C , 20000 $\times g$, 10 min) the supernatant was collected and hydrolyzed at 60°C for 30 min using 100 μ L of 0.6 M potassium hydroxide in MeOH/water (75/25; v/v). Afterwards samples were neutralized (pH=6) with acetic acid (HOAc), diluted with 2 mL of 0.1 M disodium hydrogen phosphate buffer (adjusted to pH 6 with HOAc) and loaded onto pre-conditioned SPE cartridges. The extraction of oxylipins with the anion exchange Bond Elut Certify II SPE cartridges (200 mg, 3 mL, Agilent, Waldbronn, Germany) was carried out as described in Rund *et al.* 2017 (Anal Chim Acta 1037, 63-74). Oxylipins were eluted with ethyl acetate/*n*-hexane/acetic acid (75/25/1, v/v/v) into a tube containing 6 μ L of 30% glycerol in MeOH. After evaporation (vacuum concentrator, 30°C , 1 mbar; Christ, Osterode, Germany) the residue was reconstituted in 50 μ L MeOH containing 40 nM of each, 1-(1-(ethylsulfonyl)piperidin-4-yl)-3-(4-(trifluoromethoxy)phenyl)urea, 12-(3-adamantan-1-yl-ureido)-dodecanoic acid, 12-oxo-phytodienoic acid and aleuritic acid, as IS2 to calculate the extraction efficiency of the deuterated IS.

Table S1: Composition of master mixes. Analytes are listed according to their molecular weight and retention time

molecular mass [Da]	precursor fatty acid	analyte	t _R [min]	Master								
				I (ALA/ LA II) *	II (LA/ ALA II) *	III (ARA)	IV (ARA II)	V (EPA) *	VI (DHA) *	VII (DHA/ EPA II) *	VIII (DGLA / ARA III)	IX (Div) *
266.4	ARA	tetranor-12-HETE	14.76			X						
280.4	ARA	12-HHTrE	15.64			X						
292.4	ALA	9-OxoOTrE	18.23	X								
	ALA	13-OxoOTrE	18.03		X							
294.4	ALA	9-HOTrE	16.89	X								
	ALA	13-HOTrE	17.25	X								
	LA	13-oxo-ODE	20.47		X							
	LA	9-oxo-ODE	20.75		X							
	GLA	13-γ-HOTrE	13.36									X
	ALA	9(10)-EpODE	20.03	X								
	ALA	12(13)-EpODE	20.48	X								
	ALA	15(16)-EpODE	19.86	X								
	LA	9(10)-EpOME	22.49		X							
	LA	12(13)-EpOME	22.28		X							
296.5	LA	9-HODE	19.37		X							
	LA	10-HODE	19.18									X
	LA	12-HODE	18.86		X							
	LA	13-HODE	19.26	X								
	LA	15-HODE	18.06		X							
298.5	Oleic	9(10)-Ep-stearic acid	24.03									X
312.5	ALA	9,10-DiHODE	12.74	X								
	ALA	12,13-DiHODE	12.85	X								
	ALA	15,16-DiHODE	12.68	X								
314.5	LA	9,10-DiHOME	14.92		X							
	LA	12,13-DiHOME	14.46		X							

Table S1: Continued

318.5	ARA	5-oxo-ETE	22.94								X	
	ARA	12-oxo-ETE	21.47								X	
	ARA	15-oxo-ETE	20.80								X	
	EPA	8(9)-EpETE	21.24					X				
	EPA	11(12)-EpETE	21.06							X		
	EPA	14(15)-EpETE	20.89					X				
	EPA	17(18)-EpETE	20.13					X				
	EPA	5-HEPE	19.06					X				
	EPA	8-HEPE	18.38							X		
	EPA	9-HEPE	18.73							X		
	EPA	11-HEPE	18.58					X				
	EPA	12-HEPE	18.17					X				
	EPA	15-HEPE	18.07							X		
	EPA	18-HEPE	17.34					X				
320.5	ARA	8(9)-EpETrE	23.25				X					
	ARA	11(12)-EpETrE	23.07			X						
	ARA	14(15)-EpETrE	22.50			X						
	ARA	5-HETE	21.62			X						
	ARA	8-HETE	20.97			X						
	ARA	9-HETE	21.35				X					
	ARA	11-HETE	20.57				X					
	ARA	12-HETE	21.02				X					
	ARA	15-HETE	20.02			X						
	ARA	16-HETE	18.77			X						
	ARA	17-HETE	18.61				X					
	ARA	18-HETE	18.37			X						
	ARA	19-HETE	17.78			X						
	ARA	20-HETE	18.03				X					

Table S1: Continued

322.5	DGLA	14(15)-EpEDE	23.62									X
	DGLA	5-HETrE	23.62								X	
	DGLA	8-HETrE	21.76								X	
	DGLA	12-HETrE	21.98									X
	DGLA	15-HETrE	21.43									X
326.4	ARA	2,3-dinor-15-(<i>R,S</i>)-15-F _{2t} -IsoP	5.14			X						
328.4	ALA	9,10,11-TriHODE	7.87	X								
	ALA	9,12,13-TriHODE	6.80		X							
	ALA	9,10,13-TriHODE	6.80	X								
330.5	LA	9,10,11-TriHOME	9.24		X							
	LA	9,12,13-TriHOME	7.87		X							
	LA	9,10,13-TriHOME	8.01		X							
332.4	EPA	PGB ₃	10.02					X				
334.4	ARA	12-oxo LTB ₄	14.82				X					
	ARA	PGJ ₂	11.56				X					
	ARA	PGB ₂	11.77			X						
	ARA	20-carboxy ARA	16.90				X					
336.5	ARA	8(<i>S</i>),15(<i>S</i>)-DiHETE	12.88			X						
	ARA	5(<i>S</i>),15(<i>S</i>)-DiHETE	13.32			X						
	ARA	5(<i>S</i>),12(<i>S</i>)-DiHETE	14.30			X						
	ARA	LTB ₄	13.79				X					
	ARA	6- <i>trans</i> -LTB ₄	13.30				X					
	ARA	5(<i>S</i>),6(<i>R</i>)-DiHETE	17.13								X	
	ARA	5(<i>S</i>),6(<i>S</i>)-DiHETE	18.00								X	
	ARA	6- <i>trans</i> -12- <i>epi</i> LTB ₄	13.39								X	
	EPA	5,6-DiHETE	15.5					X				
	EPA	8,9-DiHETE	14.66					X				
	EPA	11,12-DiHETE	12.29					X				
	EPA	14,15-DiHETE	14.06					X				
	EPA	17,18-DiHETE	13.42					X				

Table S1: Continued

338.4	ARA	18-carboxy dinor LTB ₄	4.32								X	
	ARA	5,6-DiHETrE	18.00				X					
	ARA	8,9-DiHETrE	17.11				X					
	ARA	11,12-DiHETrE	16.48				X					
	ARA	14,15-DiHETrE	15.69				X					
	DGLA	LTB ₃	15.94								X	
342.5	DHA	4-oxo DHA	23.33							X		
	DHA	17-oxo DHA	21.07							X		
344.4	DHA	7(8)-EpDPE	23.18						X			
	DHA	10(11)-EpDPE	22.98							X		
	DHA	13(14)-EpDPE	22.87						X			
	DHA	16(17)-EpDPE	22.78							X		
	DHA	19(20)-EpDPE	22.29						X			
	DHA	4-HDHA	22.17							X		
	DHA	7-HDHA	21.25							X		
	DHA	8-HDHA	21.47						X			
	DHA	10-HDHA	20.78						X			
	DHA	11-HDHA	21.12									X
	DHA	13-HDHA	20.52						X			
	DHA	14-HDHA	20.79									X
	DHA	16-HDHA	20.21									X
	DHA	17-HDHA	20.35							X		
	DHA	20-HDHA	19.67						X			
	n3-DPA	17-oxo DPA	22.26									X
352.5	ARA	15-oxo-15-F _{2t} -IsoP	7.62			X						
	ARA	20-OH-LTB ₄	6.10			X						
	ARA	LXA ₄	9.74			X						
	EPA	PGF _{3α}	6.88								X	
	EPA	15-F _{3t} -IsoP	5.94									X

Table S1: Continued

354.5	ARA	PGF _{2a}	8.08				X					
	ARA	15-F _{2t} -IsoP	7.33				X					
	ARA	13,14-dihydro-15-oxo-15-F _{2t} -IsoP	5.25								X	
	ARA	5(R,S)-5-F _{2t} -IsoP	7.57				X					
	ARA	5(R,S)-5-F _{2c} -IsoP	9.54				X					
356.5	DGLA	PGF _{1a}	8.13								X	
	DGLA	15-F _{1t} -IsoP	7.04								X	
360.5	DHA	RvD5	13.59							X		
	DHA	MaR2	15.09							X		
	DHA	PDx	13.51						X			
362.5	DHA	7,8-DiHDPE	17.84						X			
	DHA	10,11-DiHDPE	17.04						X			
	DHA	13,14-DiHDPE	16.67						X			
	DHA	16,17-DiHDPE	16.40						X			
	DHA	19,20-DiHDPE	15.76						X			
	n3-DPA	7(S),17(S)-diH DPA	14.06									X
366.5	ARA	20-COOH-LTB ₄	5.87			X						
368.5	EPA	d17-6-keto-PGF _{1a}	5.17					X				
370.5	ARA	6-keto-PGF _{1a}	5.85			X						
376.5	DHA	RvD4	11.17						X			
382.5	AdA	1a,1b-dihomo-PGF _{2a}	10.63									X

*Isoprostanes and isofuranes may be added to the master mixes, as described in Rund *et al.*, 2017 Anal Chim Acta 1037, 63-74

Table S2: Pipetting scheme for the sequential dilution of the standard series

Calibrant number	Concentration level [nM]	final volume [mL]	Volume of standard [mL]	standard	Volume of IS Master [μL]	concentration IS [nM]
OXY 16	500	50	2.5	all Masters	200	20
OXY 15	250	20	10	OXY 16	40	20
OXY 14	100	50	10	OXY 16	160	20
OXY 13	50	50	5	OXY 16	180	20
OXY 12	25	25	2.5	OXY 15	90	20
OXY 11	10	50	5	OXY 14	180	20
OXY 10	5	50	5	OXY 13	180	20
OXY 9	2.5	25	2.5	OXY 12	90	20
OXY 8	1	25	2.5	OXY 11	90	20
OXY 7	0.75	20	1.5	OXY 11	74	20
OXY 6	0.5	25	2.5	OXY 10	90	20
OXY 5	0.25	25	2.5	OXY 9	90	20
OXY 4	0.1	25	2.5	OXY 8	90	20
OXY 3	0.05	20	2	OXY 6	72	20
OXY 2	0.025	20	2	OXY 5	72	20
OXY 1	0.01	20	2	OXY 4	72	20

Table S3: Parameters of the LC-ESI(-)-MS/MS method. Shown are transitions for each analyte for quantification in scheduled single reaction monitoring (SRM) mode, MS potentials (declustering potential (DP), entrance potential (EP), collision energy (CE), cell exit potential (CEP)), assigned internal standards (IS), retention time (t_R), full width at half maximum (FWHM), limit of detection (LOD), calibration range with lower limit of quantification (LLOQ) and upper limit of quantification (ULOQ), slope and correlation coefficient of the calibration curve (r^2).

- 1) full peak width at half maximum (FWHM) determined as mean width of standards (0.25 - 5 nM)
- 2) limit of detection (LOD) set to lowest concentration with a signal to noise ratio ≥ 3
- 3) lower limit of quantification (LLOQ) set to lowest calibration standards with a signal to noise ratio ≥ 5 and accuracy $\pm 20\%$
- 4) upper limit of quantification (ULOQ) set to calibration of the highest injected standard
- 5) calibration was performed as weighted regression using $1/x^2$ weighting
- 6) other isoprostanes, isofuranes and phytoprostanes can be included as described in Rund et al., 2017 (Anal Chim Acta 1037, 63-74)

Table S4: Statistical analysis of the effects of additives on the apparent oxylipin pattern.
Statistical differences between “no additive” and different additives were evaluated by two-way ANOVA followed by Bonferroni post-test.

	anti-ox mix	BHT	EDTA	IND	t-AUCB
	<i>p-val</i>				
5-HETE	p <0.05	p <0.05	ns	ns	ns
9-HETE	p <0.01	p <0.01	ns	ns	ns
12-HETE	p <0.05	p <0.01	ns	ns	ns
15-HETE	p <0.001	p <0.001	ns	ns	ns
20-HETE	ns	ns	ns	ns	ns
5-HEPE	ns	p <0.05	ns	ns	ns
12-HEPE	p <0.01	p <0.01	ns	ns	ns
15-HEPE	p <0.05	p <0.001	ns	ns	ns
18-HEPE	p <0.001	p <0.001	ns	ns	ns
4-HDHA	p <0.001	p <0.001	ns	ns	ns
7-HDHA	ns	ns	ns	ns	ns
14-HDHA	p <0.01	p <0.01	ns	ns	ns
17-HDHA	p <0.001	p <0.001	ns	ns	ns
13-HODE	p <0.05	p <0.05	ns	ns	ns
13-HOTrE	ns	ns	ns	ns	ns
5(6)-EpETrE	ns	ns	ns	ns	ns
8(9)-EpETrE	ns	ns	ns	ns	ns
11(12)-EpETrE	ns	ns	ns	ns	ns
14(15)-EpETrE	ns	ns	ns	ns	ns
17(18)-EpETE	ns	p <0.05	ns	ns	ns
19(20)-EpDPE	ns	ns	ns	ns	ns
12(13)-EpOME	ns	ns	ns	ns	ns
15(16)-EpODE	ns	ns	ns	ns	ns
14,15-DiHETrE	ns	ns	ns	ns	ns
17,18-DiHETE	ns	ns	ns	ns	ns
19,20-DiHDPE	ns	ns	ns	ns	ns
12,13-DiHOME	ns	ns	ns	ns	ns
15,16-DiHODE	ns	ns	ns	ns	ns

Table S5: Oxylipin concentrations in quality standard (QS) plasma. Shown are analyzed oxylipins sorted by their retention time (tR) with their mass transitions used for quantification in scheduled SRM mode, limit of detection (LOD) and calibration range with lower limit of quantification (LLOQ) and upper limit of quantification (ULOQ) in vial. For each analyte mean \pm SD (n=8) concentration in plasma and ratio of determined concentration to LLOQ (fold LLOQ) was calculated. Plasma samples are concentrated during sample preparation by factor 2 yielding lower LLOQ in human plasma. The LLOQ is provided in grey when concentration of analyte was <LLOQ in more than 50% of the samples.

Table S6: Analyte concentrations of total oxylipins in human EDTA plasma during the transitory stage. Shown are mean \pm SD concentrations for all storage conditions and times as well as for the QS plasma. Additionally, for each analyte lower limit of quantification (LLOQ) is displayed. When analyte concentration was <LLOQ in more than 50% of the samples the LLOQ (highlighted in grey) is shown instead of mean.

Table S7: Analyte concentrations of total oxylipins during long-term storage of human EDTA plasma. Shown are mean concentrations of oxylipins >LLOQ for all storage times. In addition, a concentration range of $\pm 30\%$ (corresponds to the analytical variance) was determined for each oxylipin based on the concentration quantified in month 1.

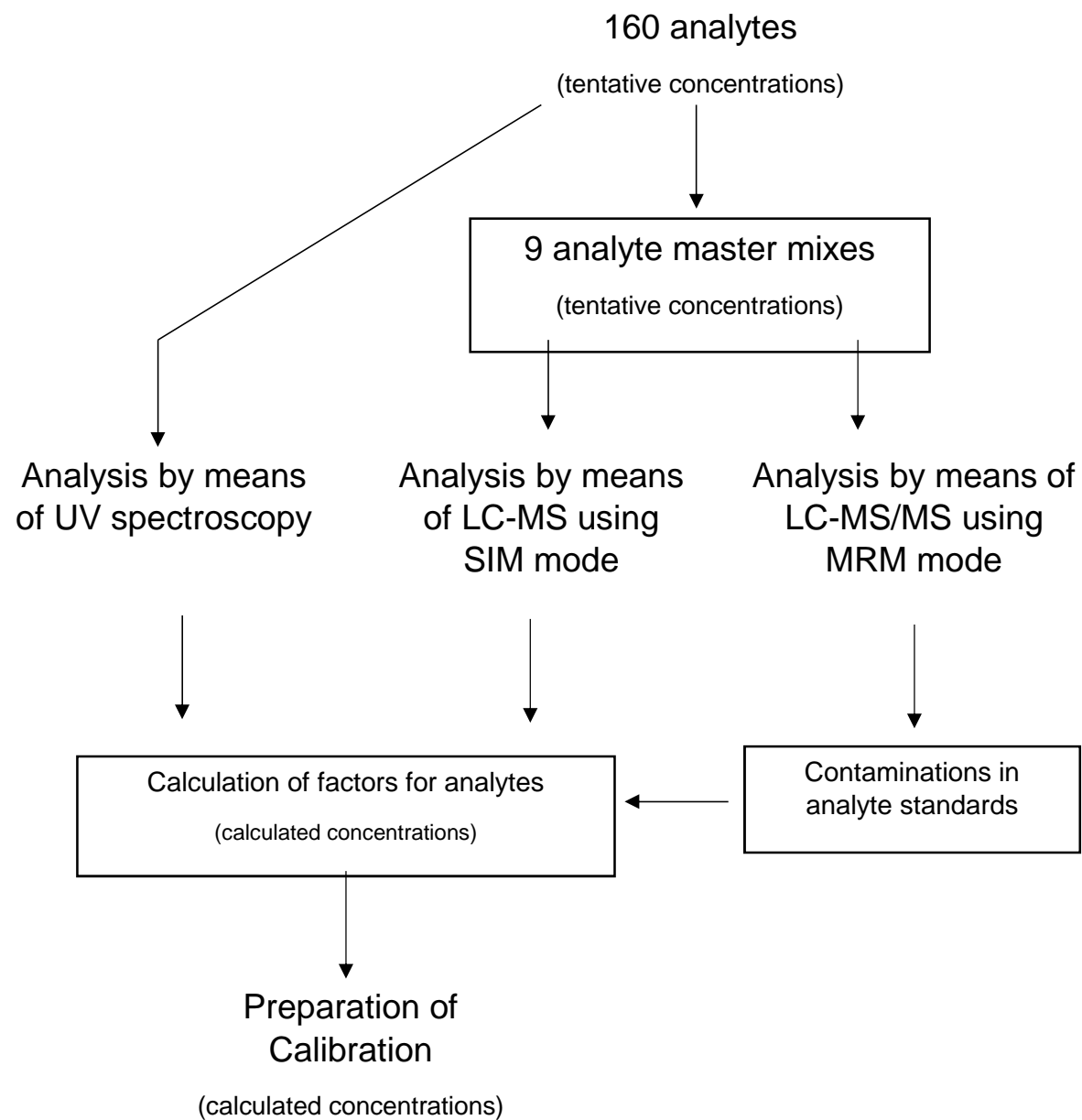


Figure S1: Scheme to generate an oxylipin multi-analyte standard series with characterized purity and concentration.

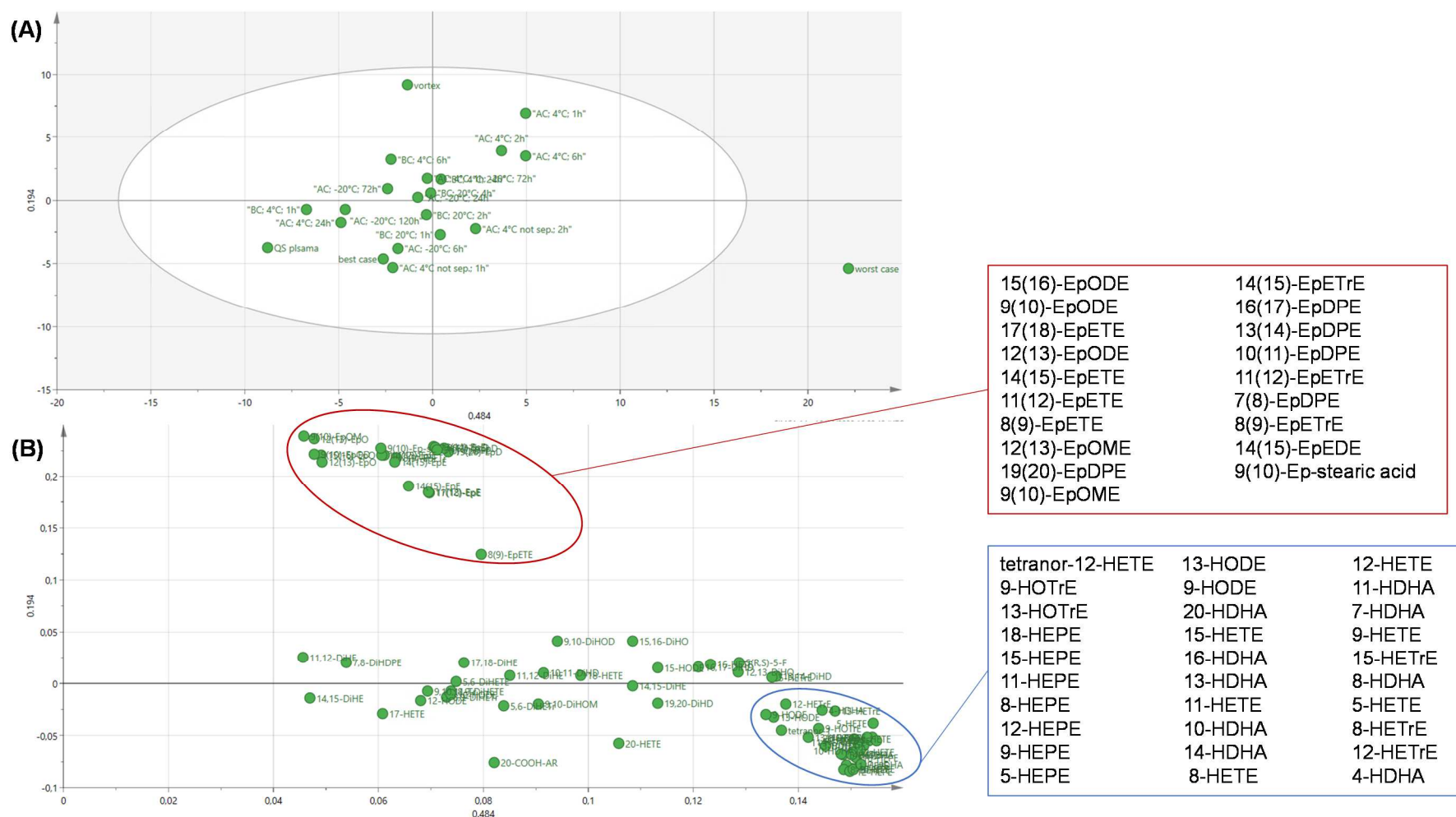


Figure S2: Principal components analysis (PCA) model. **A)** The score plot for 1st (48% of variability) and 2nd (19% of variability) component shows the distribution of all storage conditions and identifies the worst case sample as main contributor to the variability. **B)** The loading plot shows to what extent the different storage conditions influence the oxylipin concentrations. "Vortex" influences the concentration of epoxy-PUFA (red box) and "worst case" has a great effect on the concentration of hydroxy-PUFA (blue box).

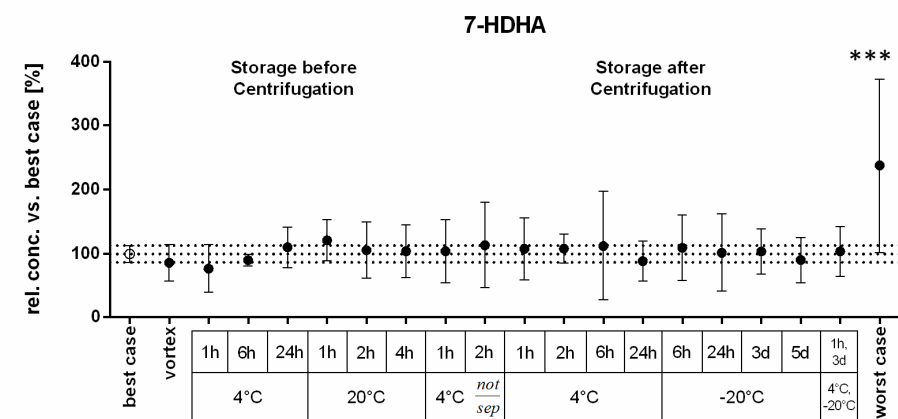
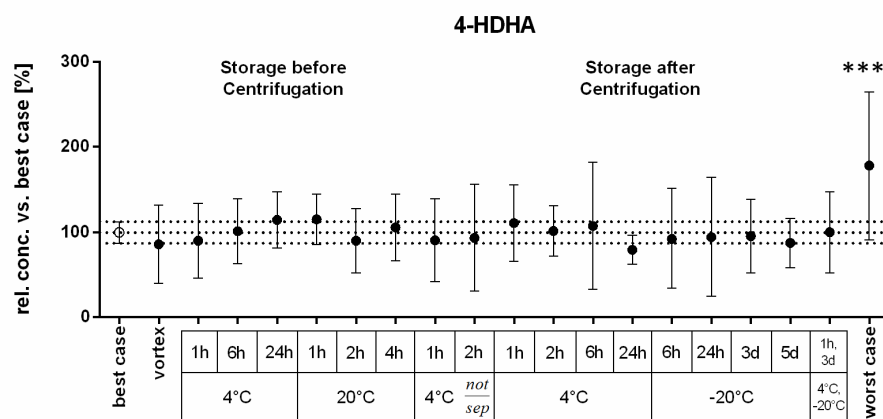
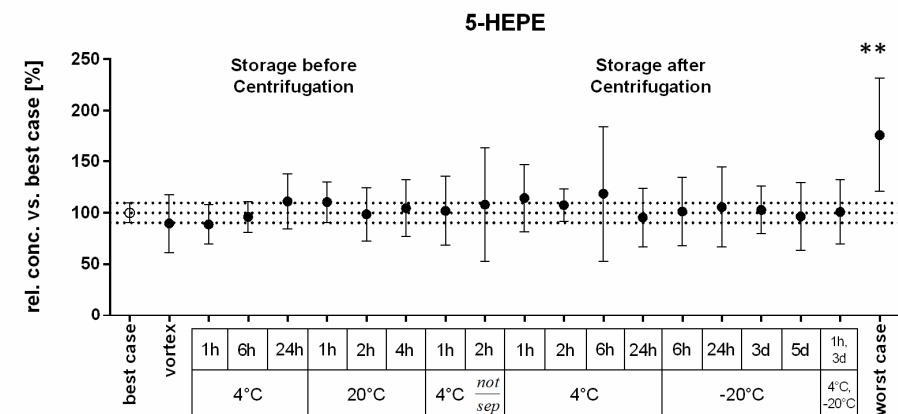
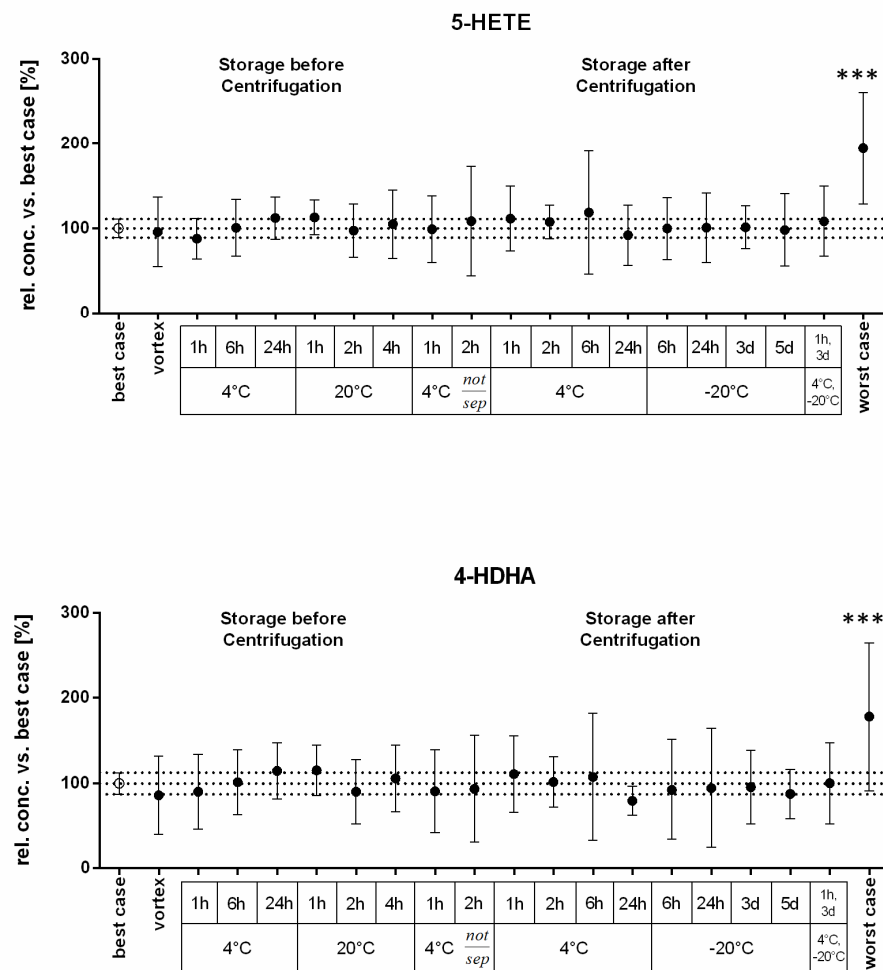


Figure S3: Concentrations of total oxylipins derived from 5-LOX pathway during the different storage conditions and times. The relative concentrations were calculated against the baseline concentration (best case sample). Shown are mean \pm 95% CI (n=4; 12 for best case). The dotted lines mark the 95% CI of the best case sample. Statistical differences between baseline and different storage conditions were evaluated by one-way ANOVA followed by Tukey post-test (** p<0.01; *** p<0.001).

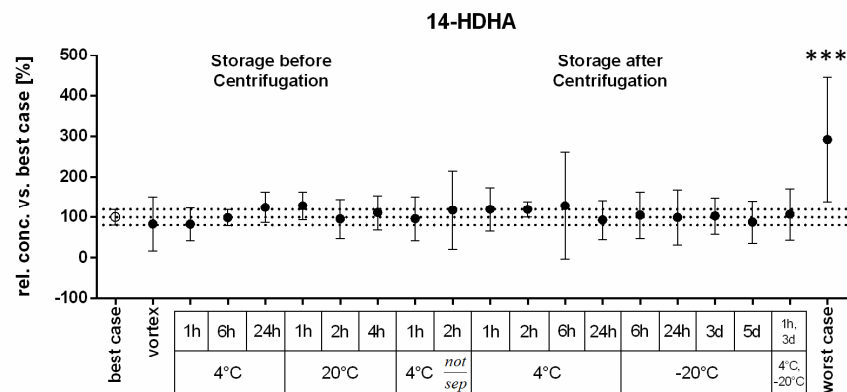
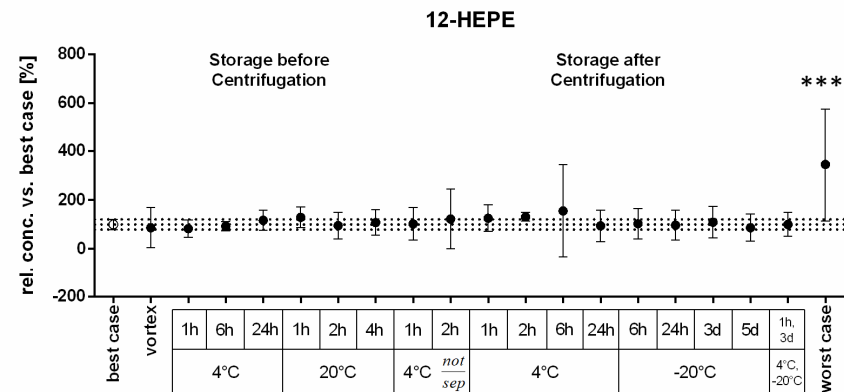
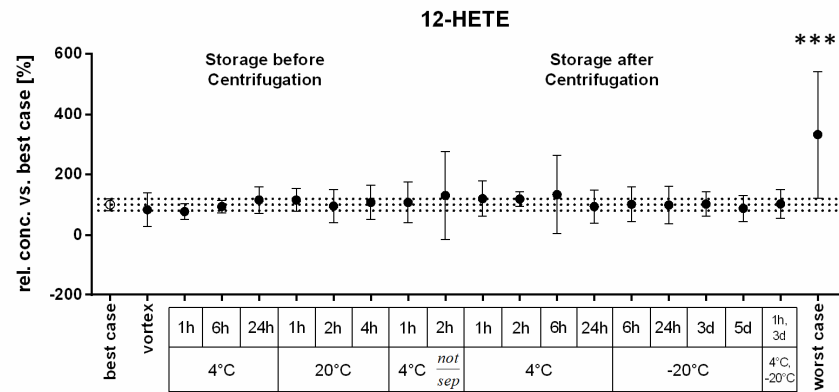


Figure S4: Concentrations of total oxylipins derived from 12-LOX pathway during the different storage conditions and times. The relative concentrations were calculated against the baseline concentration (best case sample). Shown are mean \pm 95% CI (n=4, 12 for best case). The dotted lines mark the 95% CI of the best case sample. Statistical differences between baseline and different storage conditions were evaluated by one-way ANOVA followed by Tukey post-test (***) $p < 0.001$.

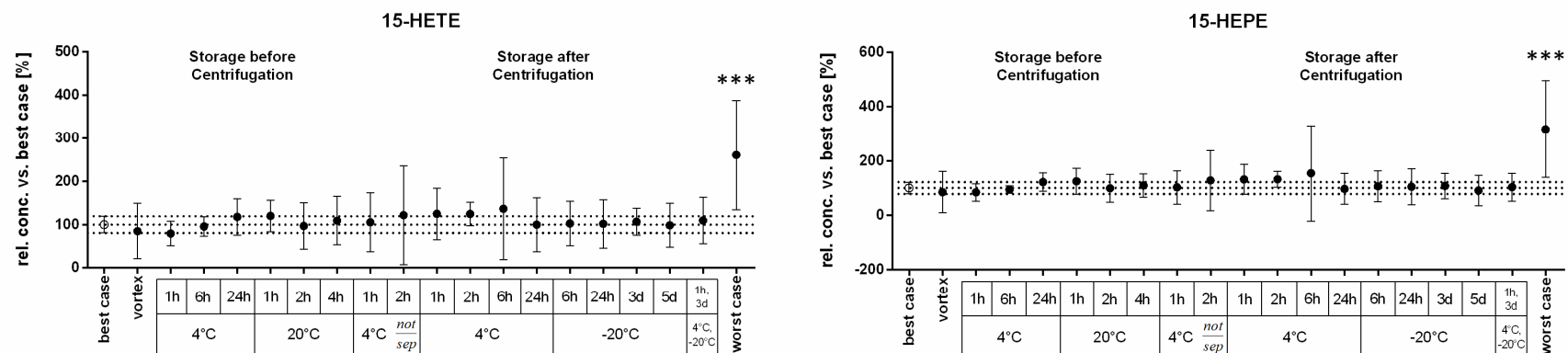


Figure S5: Concentrations of total oxylipins derived from 15-LOX pathway during the different storage conditions and times. The relative concentrations were calculated against the baseline concentration (best case sample). Shown are mean \pm 95% CI (n=4; 12 for best case). The dotted lines mark the 95% CI of the best case sample. Statistical differences between baseline and different storage conditions were evaluated by one-way ANOVA followed by Tukey post-test (***) p<0.001). Of note, the detection of 17-HDHA was not possible due to high baseline.

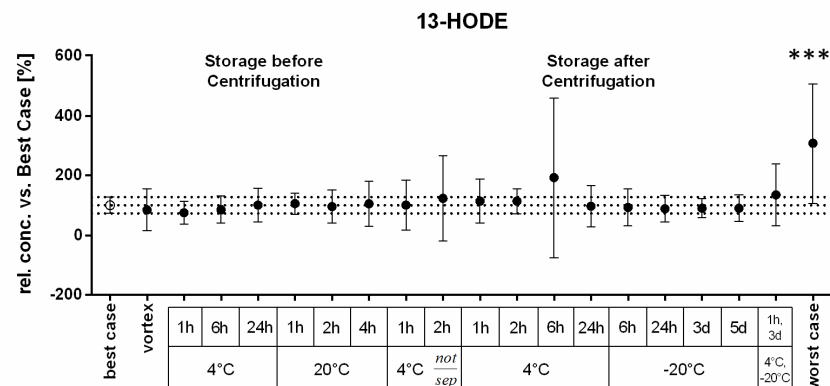
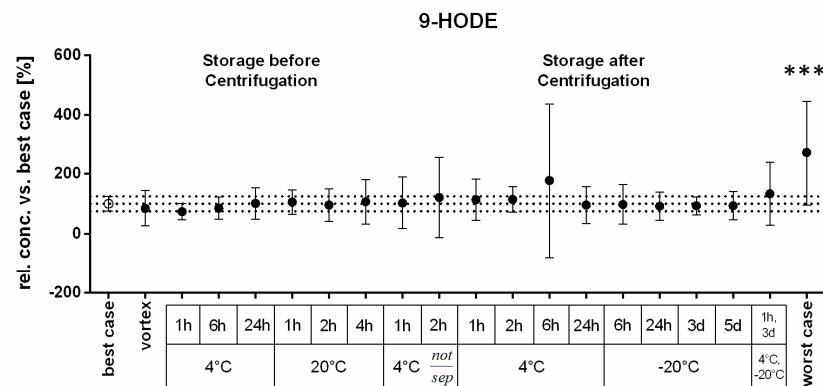
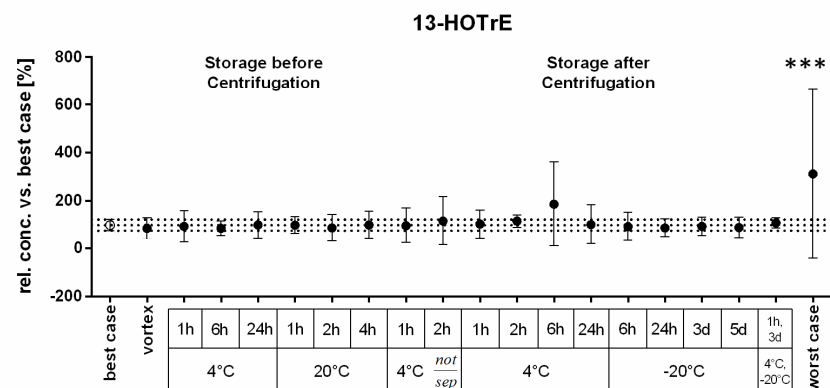


Figure S6: Concentrations of total hydroxy-PUFA derived from LA and ALA during the different storage conditions and times. The relative concentrations were calculated against the baseline concentration (best case sample). Shown are mean \pm 95% CI (n=4; 12 for best case). The dotted lines mark the 95% CI of the best case sample. Statistical differences between baseline and different storage conditions were evaluated by one-way ANOVA followed by Tukey post-test (***) p<0.001).



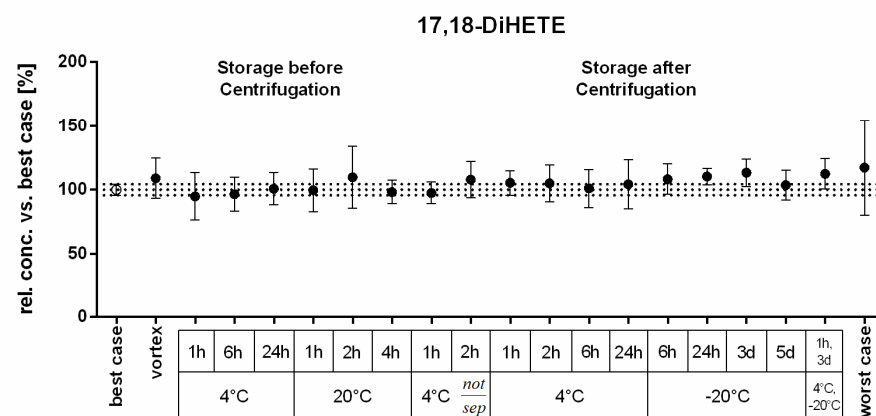
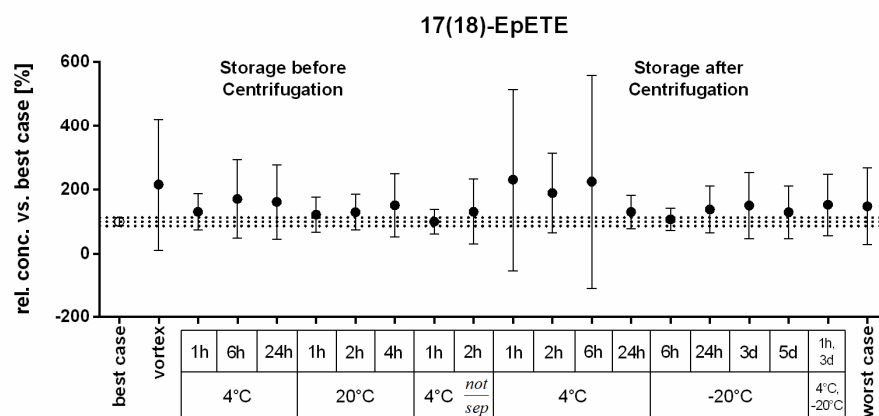
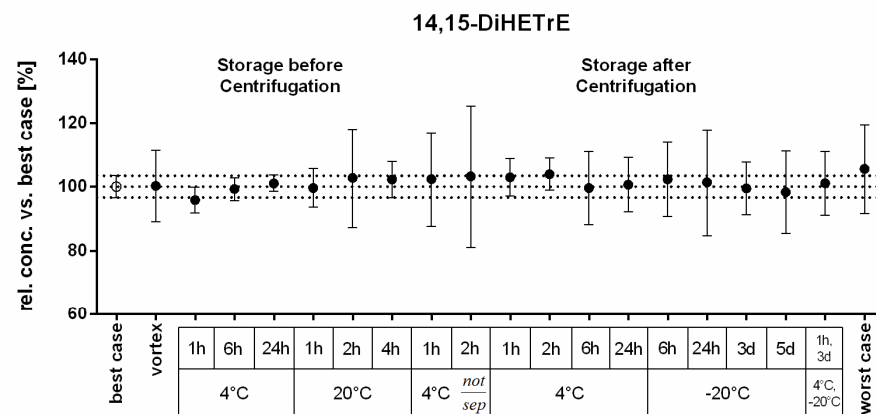
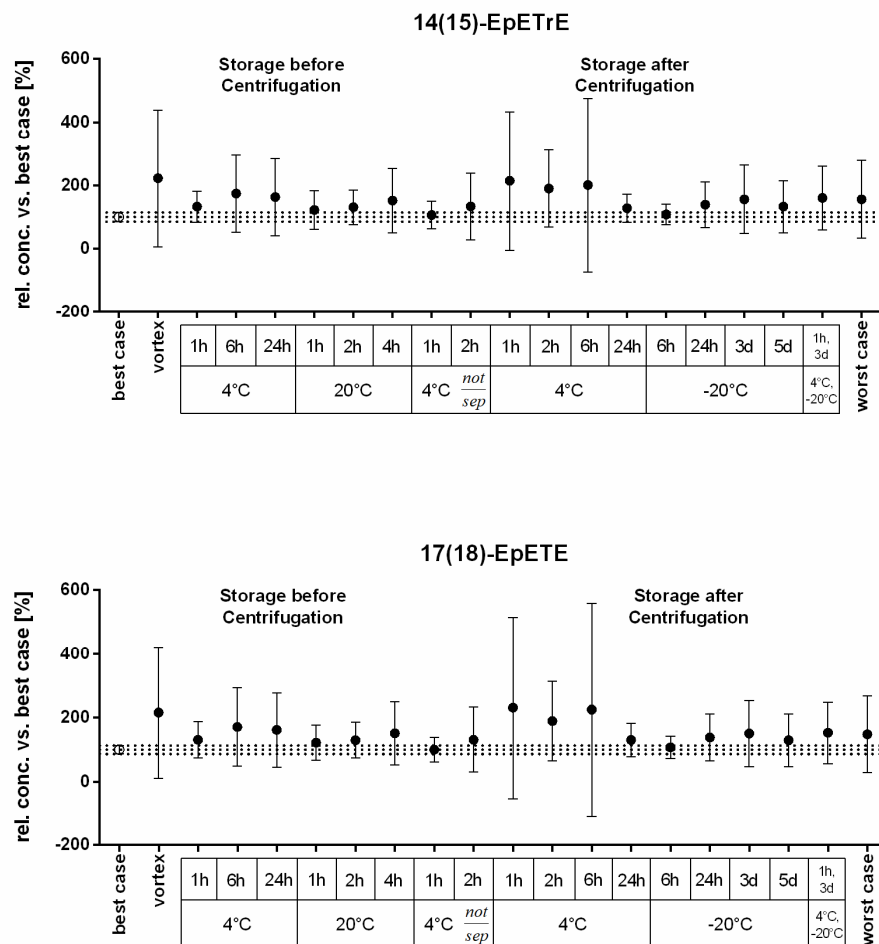


Figure S7: Concentrations of total oxylipins derived from CYP pathway during the different storage conditions and times. On the left Ep-PUFA are presented and on the right the respective *sEH* metabolites (DiH-PUFA). The relative concentrations were calculated against the baseline concentration (best case sample). Shown are mean \pm 95% CI ($n=4$; 12 for best case). The dotted lines mark the 95% CI of the best case sample. Statistical differences between baseline and different storage conditions were evaluated by one-way ANOVA followed by Tukey post-test.

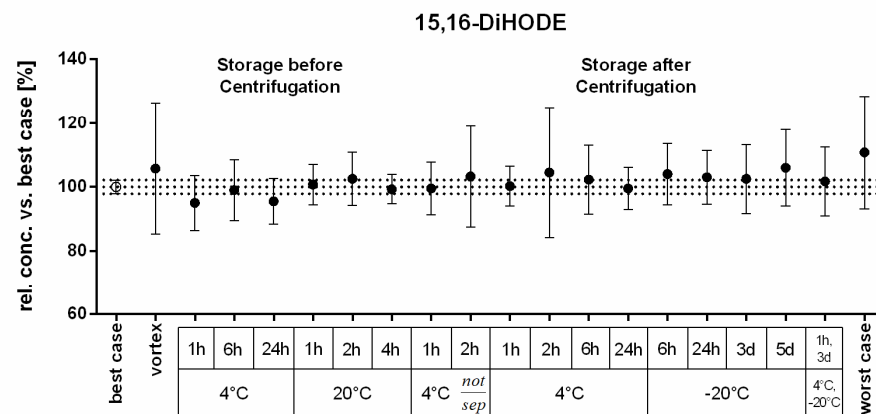
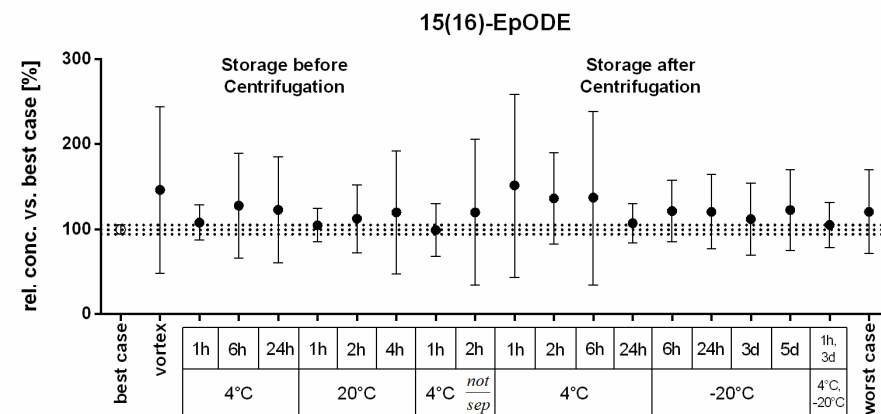
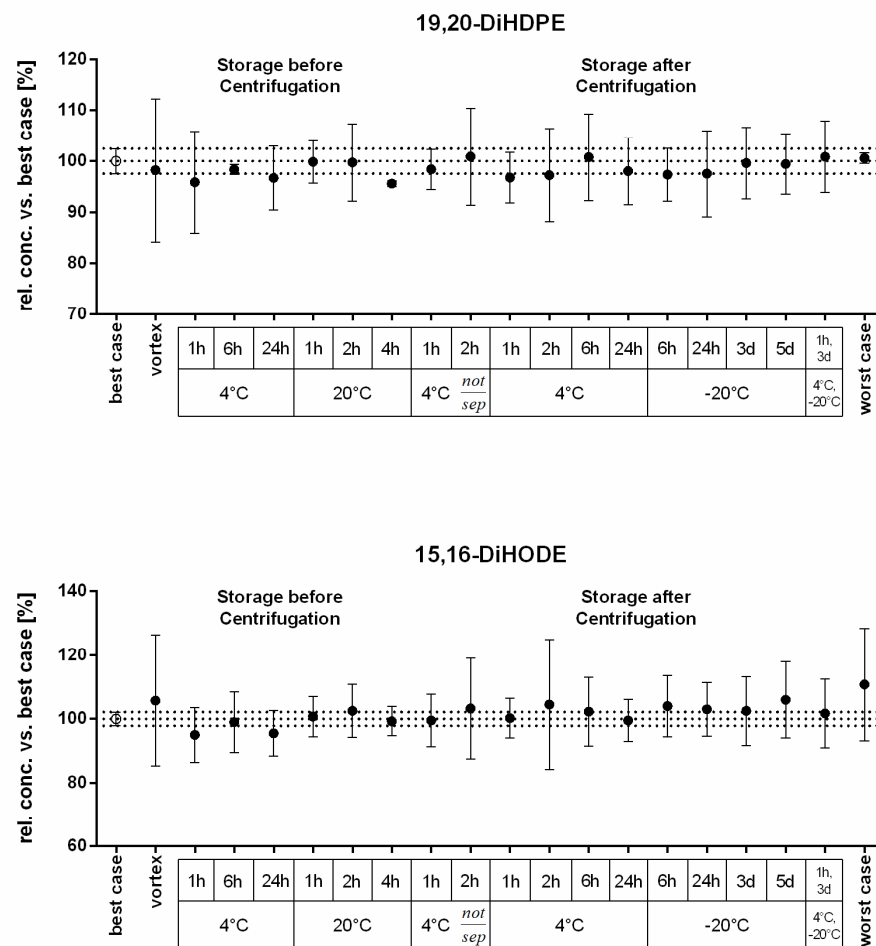
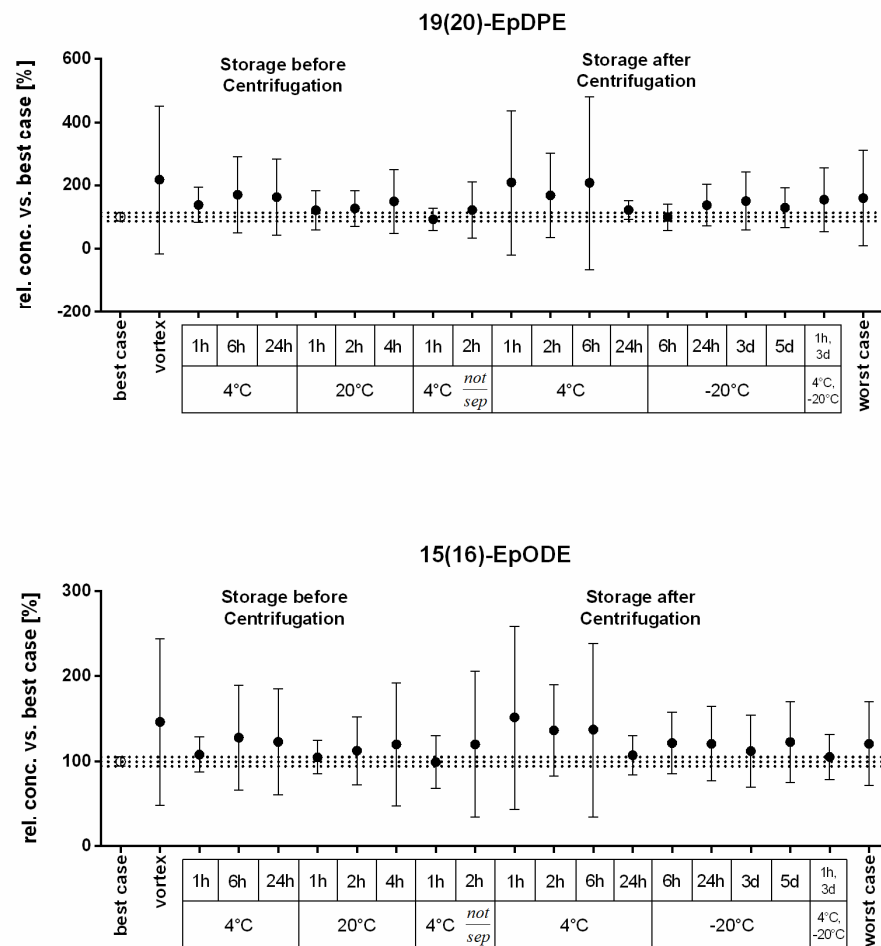


Figure S7: Continued

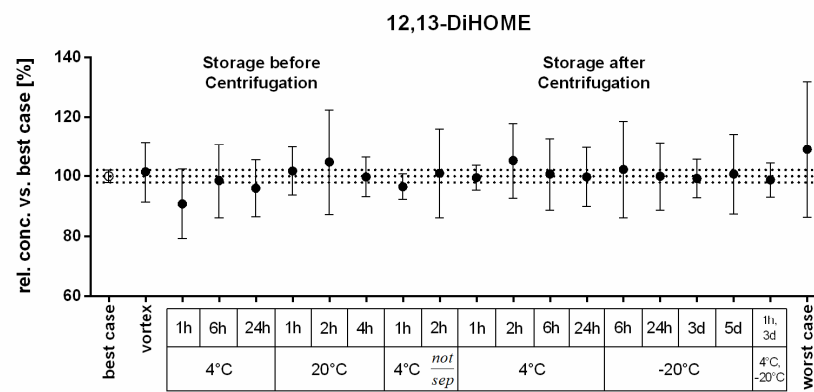
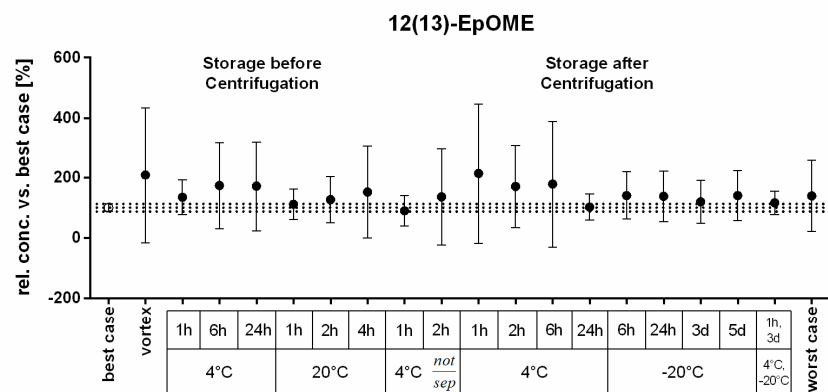


Figure S7: Continued

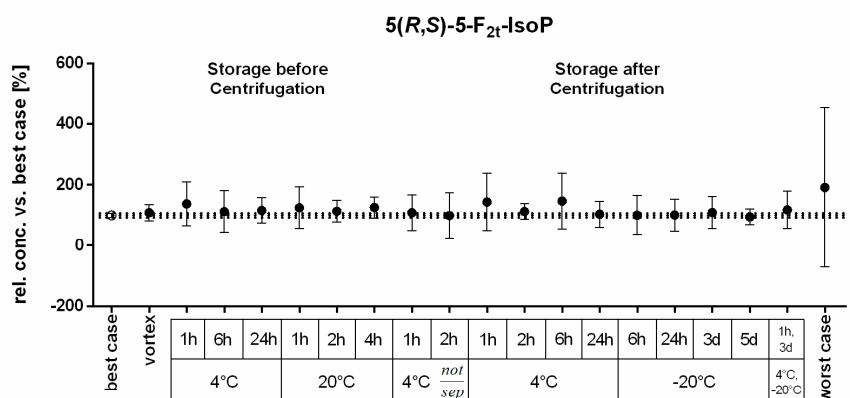
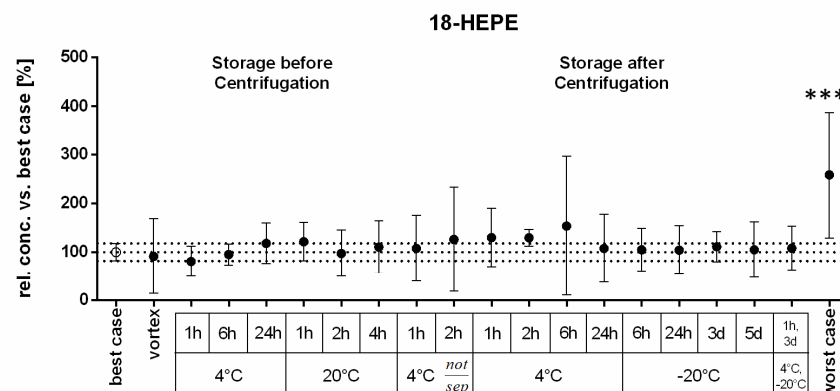
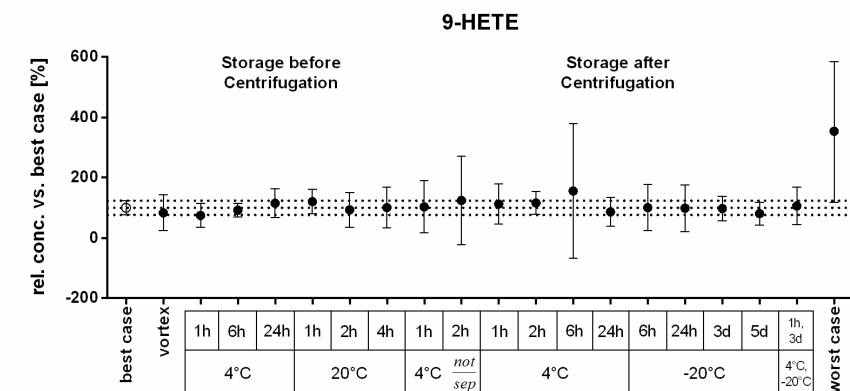


Figure S8: Concentrations of total oxylipins during the different storage conditions and times. ARA derived 9-HETE and 5(R,S)-5-F_{2t}-IsoP can be formed during autoxidation. 18-HEPE derived from EPA might be formed autoxidatively or by acetylated COX-2. The relative concentrations were calculated against the baseline concentration (best case sample). Shown are mean \pm 95% CI (n=4-12). The dotted lines mark the 95% CI of the best case sample. Statistical differences between baseline and different storage conditions were evaluated by one-way ANOVA followed by Tukey post-test (***) p<0.001).

formation pathway	before centrifugation							after centrifugation											worst case	vortex
	best case	4°C 1h	4°C 6h	4°C 24h	20°C 1h	20°C 2h	20°C 4h	4°C not sep. 1h	4°C not sep. 2h	4°C 1h	4°C 2h	4°C 6h	4°C 24h	-20°C 6h	-20°C 24h	-20°C 3d	-20°C 5d	4°C, -20°C 1h, 3d		
5-LOX	5-HETE																			
	5-HEPE																			
	4-HDHA																			
	7-HDHA																			
12-LOX	12-HETE																			
	12-HEPE																			
	14-HDHA																			
15-LOX	15-HETE																			
	15-HEPE																			
CYP	20-HETE																			
	14,15-DiHETrE																			
	17,18-DiHETE																			
	19,20-DiHDPE																			
	14(15)-EpETrE																			
	17(18)-EpETE																			
	19(20)-EpDPE																			
misc	9-HETE																			
	5(R,S)-5-F _{2t} -IsoP																			
	18-HEPE																			

variance (x)
 x < 5%
 5% < x < 10%
 x > 10%

Figure S9: Effects of the different storage conditions on the coefficient of variance (CV). The CV ($\frac{SD}{mean} * 100$) of the differently stored samples was compared to the interbatch CV of quality standard (QS) plasma (2 batches on 4 days) ($CV_{sample} - CV_{QS}$). When the difference of the sample variance is lower than 5% ($CV_{sample} < CV_{QS} + 5\%$) the sample is highlighted in green. Differences between 5% and 10% ($CV_{QS} + 5\% < CV_{sample} < CV_{QS} + 10\%$) are marked in yellow and higher than 10% ($CV_{sample} > CV_{QS} + 10\%$) in red.

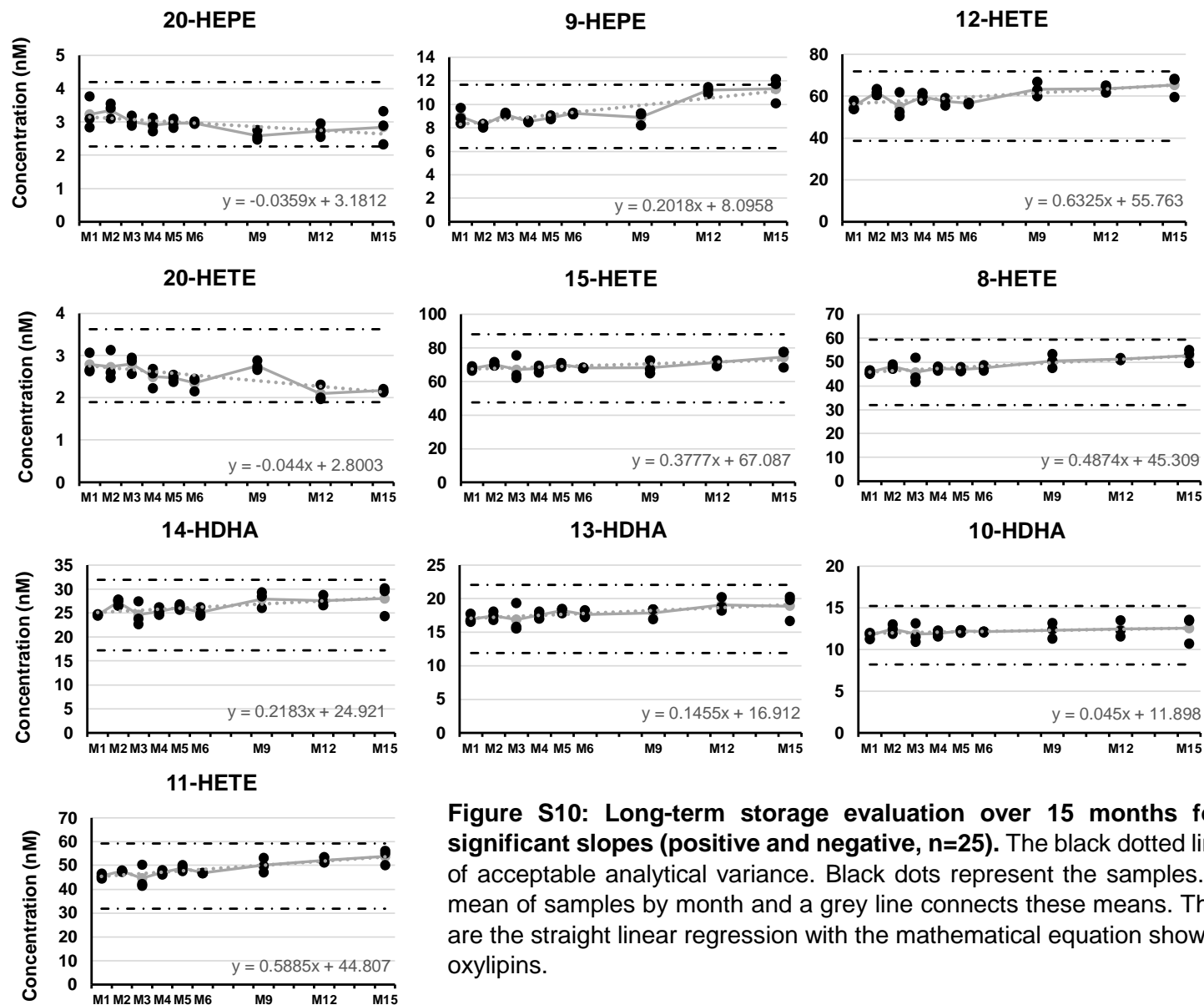


Figure S10: Long-term storage evaluation over 15 months for oxylipins with significant slopes (positive and negative, n=25). The black dotted lines mark the $\pm 30\%$ of acceptable analytical variance. Black dots represent the samples. Grey dots are the mean of samples by month and a grey line connects these means. The grey dotted lines are the straight linear regression with the mathematical equation shown near the name of oxylipins.

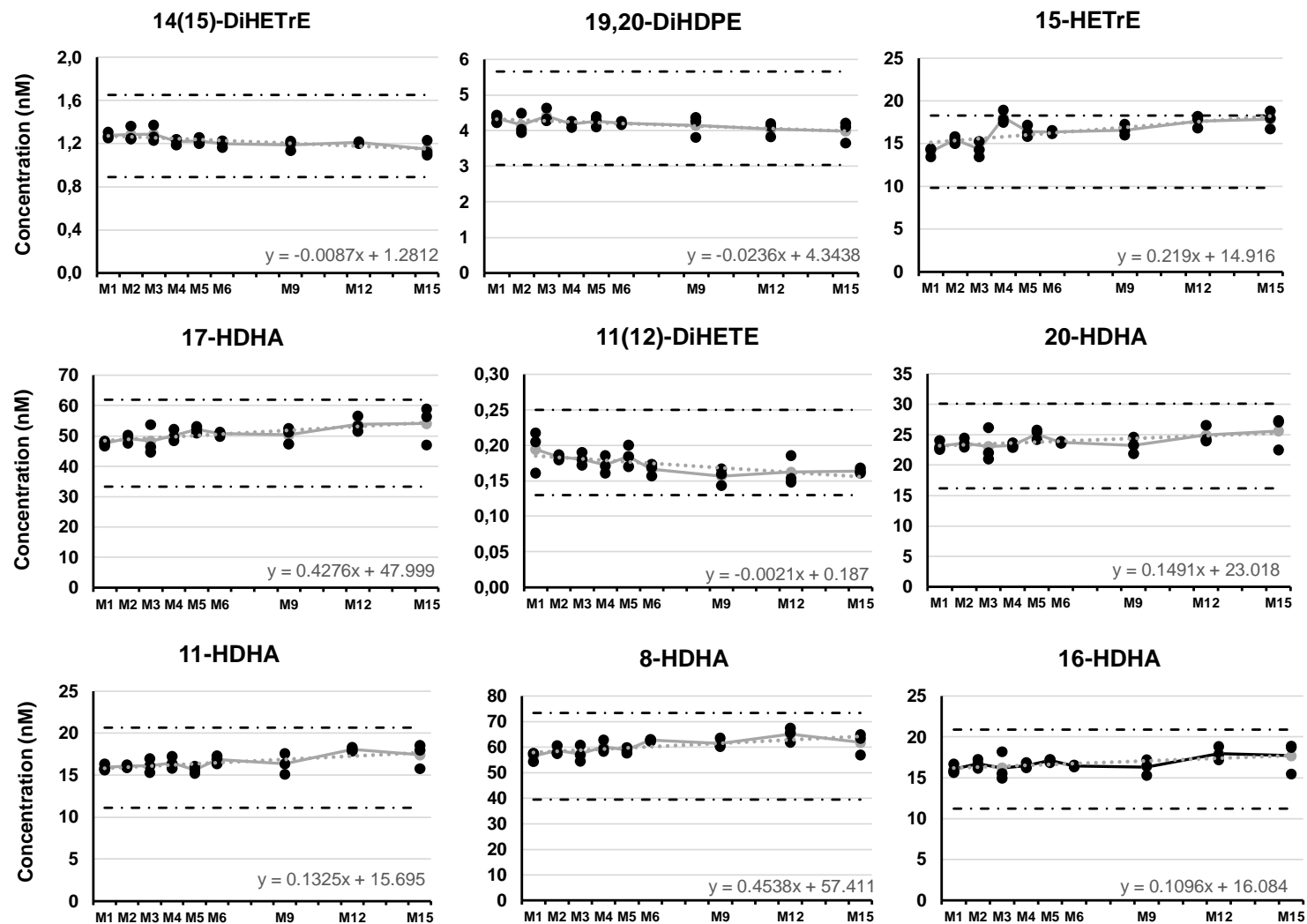


Figure S10: Continued.